ISSN 2517-7516, Membranes and Membrane Technologies, 2021, Vol. 3, No. 4, pp. 245–253. © Pleiades Publishing, Ltd., 2021.

Mathematical Modelling of a Nanoparticle Motion in a Membrane Pore under Action of Molecular Forces

V. M. Vorotyntsev[a], *, A. N. Petukhov[a], D. M. Zarubin[a], A. D. Kulikov[a], E. A. Stepanova[a], A. V. Vorotyntsev[a], and V. M. Malyshev[a]

[a] *Nanotechnology and Biotechnology Department, Nizhny Novgorod State Technical University, Nizhny Novgorod, Russia*

**e-mail: vlad@vorotyn.nnov.ru*

Received February 28, 2021; revised April 5, 2021; accepted April 9, 2021

Abstract—A mathematical model is developed to describe microfiltration on membrane filters with plane-parallel and cylindrical pores. Consideration is given to two cases of motion of Brownian particles having a radius R comparable to the radius of the filter channel a. Relations are presented for the dependence of the efficiency of particle deposition on the channel walls on the parameter $æ = Ra^{-1}$ with different values of the molecular interaction constant and with allowance for the hydrodynamic factor. The results of modeling microfiltration on membrane filters with plane-parallel and cylindrical pores are compared. It is shown that there is a qualitative agreement between the main characteristics of the microfiltration process for these two types of membrane channel cross-section. It is established that the efficiency of purification on membrane filters with cylindrical pores is considerably more significant than the efficiency attained with plane-parallel pores.

Keywords: nanoparticles, separation, ultrafiltration, nuclear filter

DOI: 10.1134/S2517751621040077

1. INTRODUCTION

There are many separation processes for the purification of gas, liquid and solid substances from nanoparticles. This is distillation [1, 2], filtration (in micro- nano- and ultrafiltration mode) [3–6] and other methods [7–10].

In [3] a classification of filtration processes depending on the pore size and pressure at the inlet and outlet of the filtration module is presented. In practice, the efficiency of nuclear filters is determined by the sieve effect, i.e. pore size determines the size of the removal particles. The driving force of membrane filtration processes is the transmembrane pressure difference [11–13]. The smaller the pore size, the greater the pressure difference is at the inlet and outlet of the membrane module, i.e. the less the pore size the greater the pressure, which depends on the capacity of the nuclear membrane filter. According to this classification micro- and ultrafiltration processes are considered. Microfiltration is a process in which membranes are used with sizes up to 100 nm, that is the highest level of nanoparticle size. The pressure difference is not very high, approximately one bar. Ultrafiltration is used for the separation of particles in the nanometer range (100–2 nm). Porosity and capacity are usually low and pressure difference varies at 1–6 bars.

In these membranes, the pore size corresponds with nanoparticle size. In microfiltration nondissolved nanoparticles with a greater size than the pore size are retained by the nuclear filter. Usually, particles for the ultrafiltration process have a smaller size than the pore size and the mechanism of this separation process is the diffusion of nanoparticles through the pores of the filter. For ultrafiltration, target components are dissolved macromolecules. In our case, nondissolved solid nanoparticles. The case is considered when the concentration of nanoparticles is small (you can ignore their interaction with each other) and their size is smaller than the pore size. In practice this is the case for the dilute solution containing a small concentration of nanoparticles and the task of high purification of liquids from nanoparticles is set. Liquids without nanoparticles are used in nanoelectronic, optoelectronic and other applications.

The settling of nanoparticles on the pore walls has, on the one hand, a positive effect, since the liquid is purified, and on the other hand, a negative effect, since the pores are clogged and the fluid flow decreases. In both cases, it is required to calculate the sedimentation of nanoparticles in the pores of the filters.

The microfiltration and ultrafiltration method is beginning to find a more widespread use for obtaining high-purity substances. In this regard, it is important

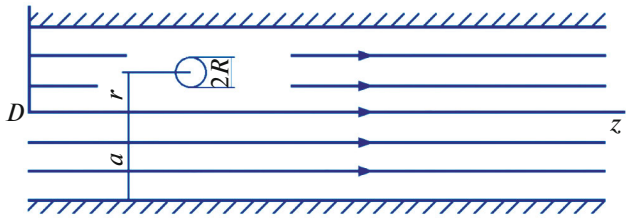

Fig. 1. Diagram of the membrane filter element channel.

to solve the problem of the effectiveness of the microfiltration method, to establish the stages that limit the separation process, as well as to establish the dependence of the separating ability of filters on the main parameters of the micro- ultrafiltration processes.

Membrane filters are most widely used for microfiltration. The "sieve effect" serves as the main contributor to the degree of purification through these types of filters. In this case, liquids are purified from particles, the size of which, as a rule, exceeds the pore size of the filter. Most often, for high purification of liquids, membrane filters with a pore size of 0.5 μm are used, and more recently, 0.1–0.2 μm. The maximum quantity for the particle size distribution curve for many liquids is in the range 0.06–0.08 μm, and in some cases even lower [10]. Making filters with pores of this size is difficult. When the liquid moves in the channel through the pores of the filter, particles from the liquid can settle on the channel walls. Thus, not only the "sieve effect," but also the diffusion purification mechanism is realized.

Therefore, this article is devoted to the development of a mathematical model for the efficient microfiltration on membrane filters with plane-parallel and cylindrical pores.

2. THEORY

In a number of works [14–20], the process of deposition of particles on the channel walls due to diffusion and sedimentation of particles under the action of van der Waals forces between condensed uncharged bodies is considered [21–23]. The magnitude of these forces depends on the ratio of the particle radius R and the transverse size of the filter pore channel a (Fig. 1). For $R \ll a$, the interaction is significant only in the immediate vicinity of the channel wall. This circumstance made it possible to take into account the action of van der Waals forces by setting a special boundary condition of a type of first-order reaction with a constant K [18, 24]. In [14, 15, 25], the case was studied when $K = \infty$ and $R/a \ll 1$. If R is comparable with a, this approximation cannot be used, therefore, in the theoretical and applied aspects of the problem under consideration, it is of interest to develop a model of the microfiltration process on membrane filters when particles move in the channel with sizes comparable to those of the filter pores.

2.1. The Plane-Parallel Channel Model

Consider a plan-parallel channel 2a wide (Fig. 1). Let $\omega(r,z)drdz$ denote the probability of finding a particle of radius R inside an infinitely small parallelepiped bounded by the planes $r \pm dr/2 = \text{const}, z \pm dz/2 = \text{const}$. A particle moving in a channel experiences collision with molecules of the medium and diffuses in it at a certain velocity. In this case, the Fokker-Planck approximation is valid, according to which the probability density $\omega(r,z)$ satisfies a diffusion-type equation [22, 26], which in the stationary case can be written as

$$Lv(r)\frac{\partial\omega}{\partial z} = \frac{\partial}{\partial r}\left[D(r)\frac{\partial\omega}{\partial r} - \frac{D(r)F(r)}{kT}\omega\right], \qquad (1)$$

where L is the maximum laminar flow rate; $D(r)$ is the particle diffusion coefficient; $F(r)$ is the Van der Waals force; k is the Boltzmann constant; T is the absolute temperature; $v(r)$ is the dimensionless function of the velocity of the flow moving in the channel; $D(r) = D_\infty f_r(r))$, where $D_\infty = kT/6\pi\mu R$ is the diffusion coefficient of a particle in an infinite medium [27]; μ is the viscosity, $f_r(r)$ is a factor that takes into account the influence of the boundary.

In [28–30], an explicit expression for the quantity $f_r(r)$ was obtained for the case when one of the channel walls is at infinity. In our case, when the particle is able to interact with both walls of the channel, this value can be specified as

$$f_r(r) = f_+ f_-; \quad f_\pm = 1 - \exp\left[-\theta_\pm\left(1+\sqrt{\theta_\pm}\right)^{-1}\right], \qquad (2)$$

where

$$\theta_\pm = (a - R \pm r)R^{-1}. \qquad (3)$$

This expression qualitatively reflects the main regularities of the interaction of a particle with the channel walls and, with an accuracy of several percent, approximates the previously obtained expression when one of the channel walls is referred to infinity.

In determining the value of $F(r)$ in equation (1), we use the Hamaker approximation for the force of attraction between a sphere and a plane [31, 32]. In our case, we define the force of interaction of the particle with the channel walls as a superposition of the forces of attraction of the particle to each of the two-channel walls separately and represent the following expression:

$$F(r) = \frac{2}{3}A\frac{R(a-R)r}{\left[(a-R)^2 - r^2\right]^2}, \qquad (4)$$

where A is the Hamaker constant.

Equation (1) is solved with boundary conditions in the form [8]:

$$\omega(r,0) = 1;\ 0 \le r < r_{m\delta}, \tag{5}$$

$$\omega(r_{m\delta}, z) = 0;\ 0 \le z \le z_K, \tag{6}$$

$$\frac{\partial\omega}{\partial r}(0,z) = 0;\ 0 \le z \le z_K, \tag{7}$$

where $r_{m\delta} = a - K - \delta$, δ is the minimum gap between the particle and the channel wall, z_K is the channel length.

Boundary condition (5) determines the probability of finding a particle at the channel entrance, condition (6) indicates the fact that along the entire length of the channel, particles located near the channel wall (the gap does not exceed δ, and the distance of the particle center from the channel axis is greater than or is equal to $r_{m\delta}$), are considered captured by the channel walls and leave the fluid flow. Condition (7) follows from the symmetry condition at $r = 0$ and the continuity of the function $\omega(r, z)$ along the channel length.

Let's move on to dimensionless variables:

$$r = au,\ z = l_d\varphi, \tag{8}$$

where $l_d = La^3\left(D_\infty R\right)^{-1} = 6\pi\mu La^3\left(kT\right)^{-1}$.

In this case, Eq. (1) with boundary conditions (5)–(7) will be written as

$$\vartheta(u)\frac{\partial\omega}{\partial\varphi} = f_r(u)\frac{\partial^2\omega}{\partial u^2} + P(u)\frac{\partial\omega}{\partial u} + Q(u)\omega, \tag{9}$$

$$\omega(u,0) = 1;\ 0 \le u < u_{m\varepsilon}, \tag{10}$$

$$\omega(u_{m\varepsilon},\ \varphi) = 0;\ 0 \le \varphi \le \varphi_K, \tag{11}$$

$$\frac{\partial\omega}{\partial u}(0,\ \varphi) = 0;\ 0 \le \varphi \le \varphi_K, \tag{12}$$

where $u_{m\varepsilon} = u_m - \varepsilon$, $u_m = 1 - \chi, \varepsilon = \delta/a$; $f_r(u) = \chi^{-1} f_+ f_-$; $\chi = Ra^{-1}$; $\theta_\pm = (1 - \chi \pm u)\chi^{-1}$; $F(u) = B\dfrac{\chi(1-\chi)u}{\left[(1-\chi)^2 - u^2\right]^2}$;

$Q(u) = -\dfrac{\partial\left[f_r(u)F(u)\right]}{\partial u}$; $P(u) = \dfrac{\partial f_r(u)}{\partial u} - f_r(u)F(u)$;

$B = \dfrac{2A}{3kT}$.

Equation (9) with boundary conditions (10)–(12) was solved numerically by the finite difference method. The considered boundary value problem has a singularity: as $u \to u_m$, the expression $f_r(u)F(u) \sim \varepsilon^{-\vartheta}$, $\vartheta > 0$; if $\varepsilon \to 0$, then $f_r(u)F(u) \to \infty$. To ensure uniform accuracy of approximation over the entire interval, a grid with a variable step was used:

$$G_{\tau h} = \{u_{i+1} = u_i + h_i,\ i = 1,\ldots,N,\ u_1 = 0,\ u_{N+1} = u_{m\varepsilon};$$
$$\varphi_j = (j-1)\tau,\ j = 1,\ldots,M,\ \varphi_M = \varphi_K,\ \tau = \text{const}\},$$

in which the value of the step h_i decreases monotonically at $i \to N$. The solution to Eq. (9) was presented in the form of a table of values of the functions $\omega(u,\ \varphi)$ at the nodes of the grid $G_{\tau h}$: $\omega(u_i, \varphi_j); (u_i, \varphi_j) \subset G_{\tau h}$.

The efficiency of particle deposition in the channel was estimated by the quantity $\bar{\omega}(\varphi)$, which at $\vartheta(u) = 1$ is equal to the probability density of finding a particle in the channel section with the plane $\varphi = \text{const}$ [10]. The value of the function $\bar{\omega}(\varphi)$ is the average concentration of particles in the channel cross section at $\varphi = \text{const}$ in the limiting case, when the particle size is small, $\chi = R/a \ll 1$, and equation (1) is the usual diffusion equation. The value of the function $\bar{\omega}(\varphi_{j+1})$ was calculated by the formula

$$\bar{\omega}(\varphi_{j+1}) = \left(2\bar{\vartheta}\right)^{-1} \times \left[\vartheta_1\omega_{1,j+1}h_1 + \sum_{i=1}^{N}\vartheta_{i+1}\omega_{i+1,j+1}\left(h_i + h_{i+1}\right)\right], \tag{13}$$

where $\bar{\vartheta} = \int_0^{u_{m\varepsilon}}\vartheta(u)\,du$; $\vartheta_i = \vartheta(u_j)$.

The model of the process of high purification of liquids from suspended nanoparticles by the microfiltration method, determined by the system of Eqs. (9)–(12), contains four dimensionless parameters: B, æ, ε, φ_K. To assess their numerical values, the following values were used: $a = 0.1$ μm, $A = 6 \times 10^{-20}$ J, $\mu = 0.6 \times 10^{-3}$ N s/m^2, $L = 0.1$ m s^{-1} which correspond to the data available in the literature on the size of the porous membrane, the characteristics of the moving flow, and the constant of van der Waals interaction [33]. The value $B = 10$, the parameter ε was taken equal to 0.05, which corresponds to the value of the minimum gap $\delta = 50$ Å.

The data on the dependence $\bar{\omega}(\varphi)$ at various values of æ are shown in Fig. 2. It is seen that with an increase in the ratio æ, the function $\bar{\omega}(\varphi)$ for different values of φ first increases, and for æ > 0.5 begins to decrease. For the convenience of analyzing this regularity of the process, as well as calculating the function $\bar{\omega}(\varphi)$, we approximate its expression:

$$\bar{\omega}(\varphi) = \omega_0 \times 10^{-\lambda\varphi}. \tag{14}$$

The parameter λ at $\varphi \ge 0.02$ practically does not depend on φ, since in the coordinates $\log\bar{\omega}(\varphi)$, φ the function is rectilinear (Fig. 3). Thus, the feature noted above in the behavior of the function $\bar{\omega}(\varphi)$ can be represented as a dependence of the parameter λ on æ (Fig. 4), which has a minimum at a certain value of $æ_{min}$. The presence of this minimum can be explained as follows. With an increase in the parameter æ ($æ < æ_{min}$), the decrease in the efficiency of the microfiltration process is mainly associated with a decrease in the particle mobility in the channel, due to

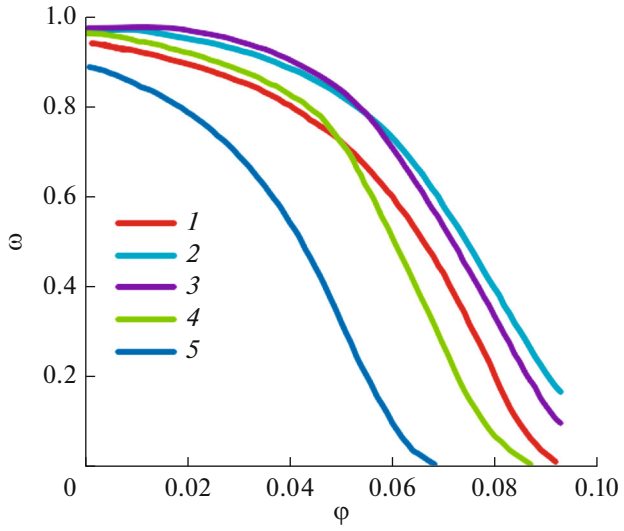

Fig. 2. Dependence of the probability density of finding a particle in the channel section with the plane φ = const on the dimensionless length of the channel at values of æ: (*1*) 0.1; (*2*) 0.5; (*3*) 0.7; (*4*) 0.9; (*5*) is the result of work [8] for æ ≪ 1.

an increase in the resistance of the medium. In this case, along with the usual influence of the medium on the nature of the particle motion in accordance with the Stokes law [34] (the factor $æ^{-1}$ in the function $f_r(u)$), an additional effect appears due to an increase in the viscosity of the medium when the particle moves near the channel wall, when æ ~ 1. For æ ≪ 1, the effect of the channel walls on the particle motion is practically excluded and the efficiency of the microfiltration process is higher (Fig. 2).

At the same time, for the case when æ ~ 1, an increase in the purification efficiency is possible due to the action of attractive forces of various nature, among which the action of van der Waals forces is mandatory. At $æ > æ_{min}$, it becomes decisive in comparison with the diffusion mechanism of microfiltration. It should be noted that a decrease in the particle path in the direction perpendicular to the channel wall ($u_m = 1 - æ \to 0$ at $æ \to 1$) also contributes to an increase in the purification efficiency. To estimate the influence of this effect, calculations were carried out for the case when $B = 0$, i.e., the action of the Van der Waals forces is negligible. In this case, no extreme point is observed for the dependence of λ on æ (Fig. 4), i.e. a decrease in the path of a particle to the channel wall with an increase in æ does not compensate for a change in the purification efficiency due to a decrease in the particle mobility. The purification efficiency does not increase.

Thus, during high purification of liquids from suspended nanoparticles, an extreme dependence of the purification efficiency on the ratio of the particle size and the filter pore channel size $R/a = æ$ is observed. Moreover, for $æ < æ_{min}$, the main contribution to the purification efficiency is made by the mechanism of diffusion movement of particles in the pores of the filter, and at values of $æ > æ_{min}$, the increase in the purification efficiency is due to the action of van der Waals forces. The $æ_{min}$ value is determined by the nature of the nanoparticle and medium, as well as by the conditions for microfiltration of liquids.

Nuclear membranes are widely used in the production of ultrapure substances by the method of microfiltration [35, 36]. These membranes differ from other

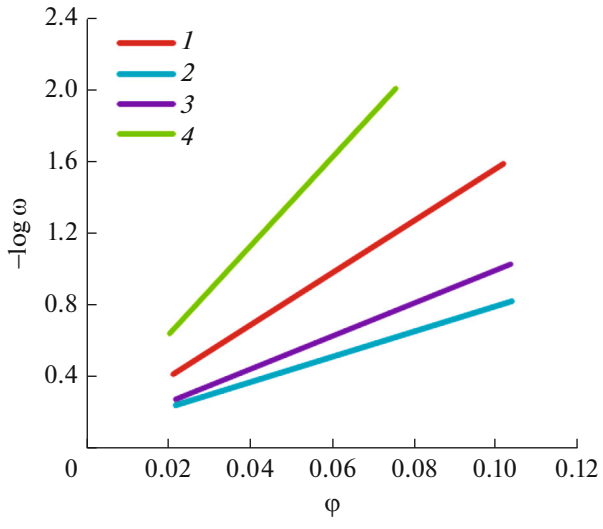

Fig. 3. Dependence of the logarithm of the probability density on the dimensionless channel length at values of æ: (*1*) 0.1. (*2*) 0.5; (*3*) 0.7; (*4*) 0.9.

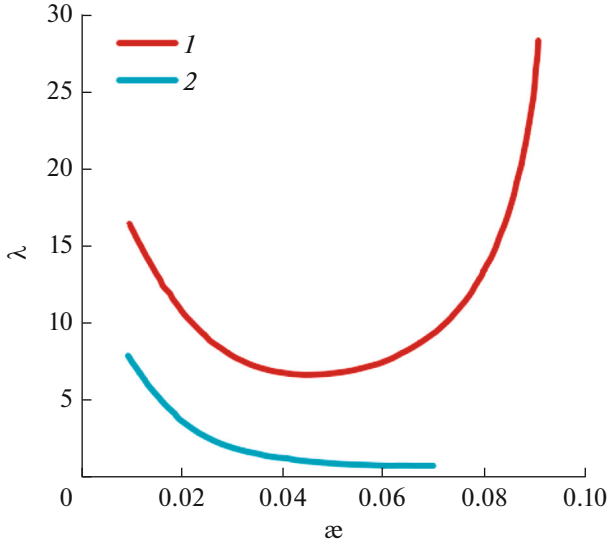

Fig. 4. Dependence of λ on the dimensionless particle radius. (*1*) $B = 10$, (*2*) $B = 0$.

types of membranes in their regular cylindrical form, their uniform structure, and the very small degree of variation in the dimensions of the pores [37, 38].

Along with the principal sieve mechanism of purification, filtration in membranes takes place by the deposition of particles on the walls of the pores of the membrane (the particle radius R being less than the radius of the pores a). In connection with this, it is important to study the mechanisms of particle deposition in these filters and establish the dependence of the separating capacity of the filter on the main parameters of the microfiltration process.

The well-known model in [39] describes particles, suspended in a fluid and ranging in size from several microns to 100 μm, through the channels of a nuclear membrane. In this case, due to the relatively large size of the particles, an approximation based on the construction of the paths of an individual particle is valid.

At the same time, for a number of fluids that are subjected to microfiltration, the maximum on the particle-size distribution curve lies within the range 0.06–0.08 μm. The deposition process in this case—when the particles behave as Brownian particles as they move in the channels—was examined in [40]. Here, the case of a membrane with plane-parallel pores was studied.

2.2. Cylindrical Channel Model

In the present investigation, we study the process of microfiltration for a membrane with cylindrical pores.

The model of the microfiltration process is described by an equation of the diffusion type. For a cylindrical channel, this equation is represented in the form:

$$L\frac{\partial\omega}{\partial z}=\frac{1}{r}\frac{\partial}{\partial r}\left[rD(r)\left(\frac{\partial\omega}{\partial r}-\omega\frac{F(r)}{kT}\right)\right], \qquad (15)$$

where r and z are the coordinates of the center of the particle along the radius and the axis of the cylindrical pore, respectively; $\omega(r,z)\times 2\pi r dr dz$ is the probability of finding a particle inside an infinitesimal volume bounded by the coordinate surfaces $r \pm dr/2 = \text{const}$, $z \pm dz/2 = \text{const}$; L is the rate of laminar flow of the fluid, which is assumed to be independent of the coordinate, r; $F(r)$ is the van der Waals force; k is the Boltzmann constant; T is the absolute temperature; $D(r) = D_\infty f_r(r)$, where D_∞ is the coefficient of diffusion of a particle in an infinite medium and $f_r(r)$ is the hydrodynamic factor. The latter accounts for the effect of the channel walls on viscous drag.

In determining $F(r)$, we will proceed on the basis of the London-Hamacker general formula for the energy of molecular interaction

$$W=-\int dv_1\int\frac{\beta q^2}{l^6}dv_2, \qquad (16)$$

where v_1 is the region of space bounded by a sphere of radius R (the particle); v_2 is all space from which we remove a cylinder of radius a of infinite length. The particle being examined is located inside the cylinder at the distance H from its surface; q is the number of atoms per unit volume of the condensed phase (spherical particle, cylindrical channel); βl^{-6} is the energy of the pairwise interactions of identical atoms in accordance with London's theory of dispersion forces [21]; l is the distance between atoms.

After performing the corresponding calculations, we reduce the six-dimensional integral (16) to the following unidimensional integral:

$$W=-\frac{AR^3}{3}\int_0^\pi\left[1+\frac{r\left(a-r\cos\varphi+2\sqrt{Q}\right)\cos\varphi}{\left(a-r\cos\varphi+\sqrt{Q}\right)^2}\right]\frac{d\varphi}{Q^{3/2}}, \qquad (17)$$

where $A=\pi^2q^2\beta$ is the Hamacker constant; $Q=a^2-2ar\cos\varphi+r^2-R^2$. Then the van der Waals force $F(r)$ is found from the relation

$$F(r)=-\frac{\partial W}{\partial r}. \qquad (18)$$

We find an asymptotic expression for the force $F(r)$ in the case when the gap H between the spherical particle and the channel wall is much smaller than the radii of curvature of the particle surface R and cylinder a.

It should be noted that at $H \ll R$, the main contribution to the integral (17) is made by values of φ close to zero (the multiplier $Q^{-3/2}\to\infty$ at $HR^{-1}\to 0$ and $\varphi\to 0$). Thus, the bracketed expression in (17) can be replaced by its value at $\varphi = 0$ and $r=a-R$. Let us now change the expression for Q. Expressing r through H by means of the relation

$$H=a-R-r, \qquad (19)$$

we obtain

$$Q=2a(1-\cos\varphi)(a-R-H)+2HR+H^2. \qquad (20)$$

In the case of small H in (20), we limit ourselves to a linear approximation Q_0 and discard the term with H^2.

Making these simplifications in (17), we obtain

$$W=-\frac{AR^2a}{3}\int_0^\pi\frac{d\varphi}{Q_0^{3/2}}. \qquad (21)$$

Calculation of the integral (21) yields [41]

$$W=-\frac{AR}{6H}\left[1-æ-H(2-æ)(2a)^{-1}\right]^{-1/2}E\left(\frac{\pi}{2},b\right), \qquad (22)$$

where $E\left(\frac{\pi}{2},b\right)$ is a complete second-order elliptic integral, $b=\left\{\left[2a(1-æ)-2H\right]\left[2a(1-æ)-H(2-æ)\right]^{-1}\right\}^{1/2}=$

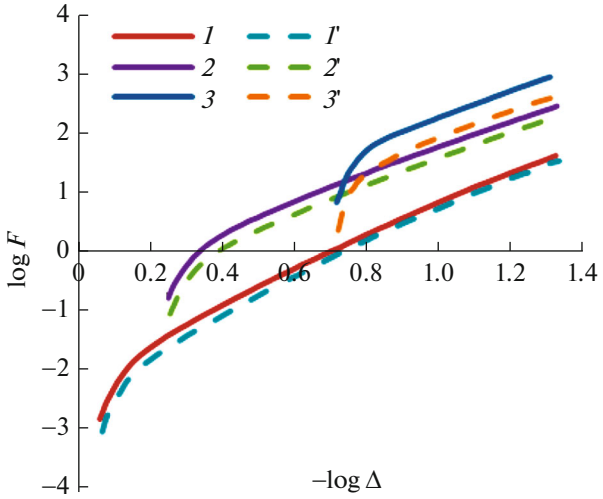

Fig. 5. Dependence of the van der Waals force on the dimensionless distance between the particle and the channel wall: æ: (*1*, *1'*) 0.1; (*2*, *2'*) 0.4; (*3*, *3'*) 0.8; $B = 2.5$. The solid line shows the relations corresponding to a membrane with cylindrical channels, while the dashed line shows the relations for a membrane with plane-parallel channels.

Ra^{-1}). When $Ha^{-1} \to 0$, $b \to 1$, $E\left(\frac{\pi}{2},1\right) = 1$, we find from (22) that

$$W = -\frac{AR}{6H\sqrt{1-æ}}. \tag{23}$$

Differentiating the right side of (23) with respect to r in accordance with (18) and allowing for (19), we obtain

$$F(r) = \frac{AR}{6H^2\sqrt{1-æ}}. \tag{24}$$

It is not hard to see that Eq. (24) coincides with the expression for force obtained from the [42] Derjaguin formula [32, 42] for the present case of molecular interaction between bodies bounded by spherical and cylindrical surfaces.

In calculating $f_h(r)$, we use an approximate formula [43] corresponding to the relation

$$f_h(r) = \frac{H_+H_-}{(H_+ + R)(H_- + R)}, \tag{25}$$

where $H_\pm = a - R \pm r$ are the maximum and minimum sizes of the gap between the sphere and the cylindrical surface of the channel. Let us change over to the dimensionless variables $u = r/a$, $\varphi = z/l_d$, where $l_d = La^3(D_\infty R)^{-1}$. Then with the same boundary conditions that were examined in [40], Eq. (15) is written in the form

$$æ\frac{\partial\omega}{\partial\varphi} = \frac{1}{u}\frac{\partial}{\partial u}\left[uf_h(u)\left(\frac{\partial\omega}{\partial u} - F(u)\omega\right)\right], \tag{26}$$

$$\omega(u,0) = 2u_{m\delta}^{-2};\ 0 \le u \le u_{m\delta}, \tag{27}$$

$$\omega(u_{m\delta},\ \varphi) = 0;\ 0 \le \varphi \le \varphi_c, \tag{28}$$

$$\frac{\partial\omega}{\partial u}(0,\ \varphi) = 0;\ 0 \le \varphi \le \varphi_c, \tag{29}$$

where $f_h(u) = \left[(1-æ)^2 - u^2\right]\left(1-u^2\right)^{-1}$; φ_c is the dimensionless length of the channel; $u_{m\delta} = 1 - æ - \delta$; δ is the dimensionless gap size at which the particle is considered to have been captured by the channel wall and

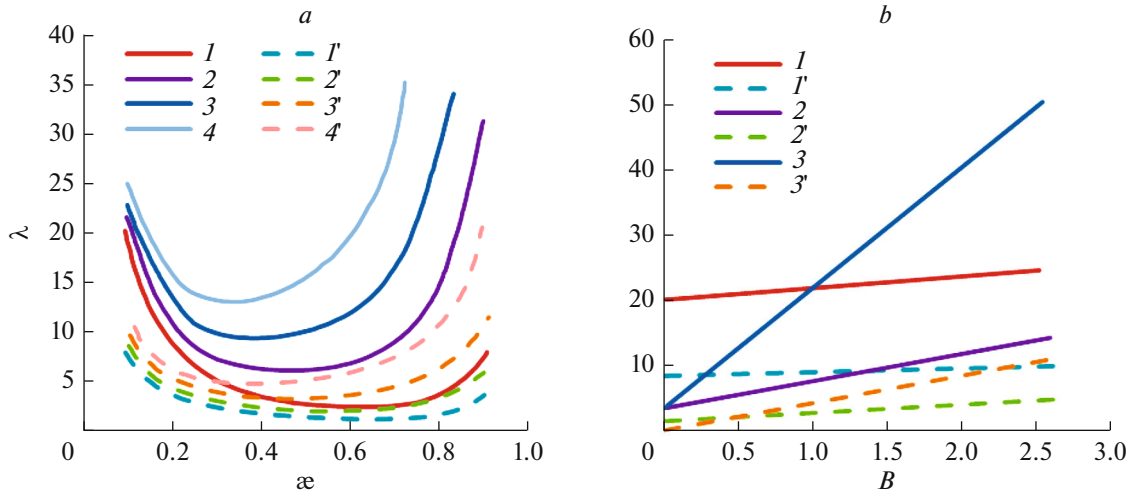

Fig. 6. Dependence of the quantity λ: (a) on the dimensionless radius of the particle æ. *B*: (*1*, *1'*) 0; (*2*, *2'*) 0.5; (*3*, *3'*) 1.25; (*4*, *4'*) 2.5; (b) on the molecular interaction constant *B*. (*1*, *1'*) æ = 0.1; (*2*, *2'*) æ = 0.4; (*3*, *3'*) æ = 0.8. The solid line shows the relations corresponding to a membrane with cylindrical channels, while the dashed line shows the relations for a membrane with plane-parallel channels.

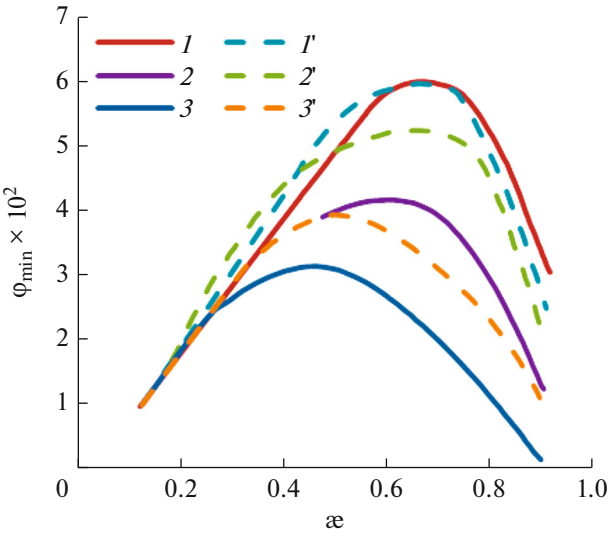

Fig. 7. Dependence of the minimum channel length φ_{min} on the dimensionless particle radius æ. *B*: (*1*, *1'*) 0; (*2*, *2'*) 0.5; (*3*, *3'*) 2.5. The solid line shows the relations corresponding to a membrane with cylindrical channels, while the dashed line shows the relations for a membrane with plane-parallel channels.

removed from the fluid flow. This parameter is introduced because at $u \to u_{m\delta}$, $f_h(u)F(u) \sim \delta^{-\vartheta}, \nu > 0$; $\delta \to 0$, then $f_h(u)F(u) \to \infty$. After differentiation of (17) in accordance with (18) and the transition to dimensionless variables, the expression for the van der Waals force is represented in the form

$$F(u) = B\text{æ}^3 \int_0^{\pi} \left\{ \frac{3 - 3u\cos\varphi - 2\text{æ}^2 + 3\sqrt{Q}}{\left(1 - u\cos\varphi + \sqrt{Q}\right)^3} \cos\varphi \right. \\ \left. - \left[1 + \frac{u\left(1 - u\cos\varphi + 2\sqrt{Q}\cos\varphi\right)}{\left(1 - u\cos\varphi + \sqrt{Q}\right)^2} \right] \frac{3(u - \cos\varphi)}{Q} \right\} \frac{d\varphi}{Q^{1/2}}, \quad (30)$$

where $B = A(3kT)^{-1}$ is the molecular interaction constant; $Q = 1 - 2u\cos\varphi + u^2 - \text{æ}^2$. If as parameter B we examine the complex Hamacker constant—which, in accordance with the London-Hamacker theory makes it possible to account for the molecular interaction of a particle with a dispersion medium [21, 32, 33]—then Eq. (30) determines the resulting van der Waals force acting on the spherical particle on the channel-wall side and on the fluid flowing in the channel. Equation (26), with boundary conditions (27)–(29), was solved by the method used in [40]. The efficiency of particle deposition in the channel was evaluated from the quantity

$$\omega_e(\varphi_c) = \int_0^{u_{m\delta}} \omega(u, \varphi_c) u du. \quad (31)$$

Numerical solution of Eqs. (26)–(29) on a computer established that purification efficiency $\omega_e(\varphi_c)$, as a function of channel length at $\varphi_c \geq \varphi_{min}$ can be approximated by an expression of the form

$$\omega_e(\varphi_c) = \omega_0 \times 10^{-\lambda\varphi_c}, \quad (32)$$

where the parameter λ is independent of φ_c; φ_{min} is the minimum channel length at which purification efficiency can still be evaluated from Eq. (32). The quantity φ_{min} was evaluated on the basis of the condition that the difference between the values of $\omega_e(\varphi_c)$, determined from Eqs. (31) and (32) not exceed 10%.

The results of the calculations are shown in Figs. 5–8; the solid line in all figures shows the relations corresponding to a membrane with cylindrical channels, while the dashed line shows the relations for a membrane with plane-parallel channels. Figure 5 presents graphs of the dependence of the van der Waals force on the value of the parameter $\Delta = 1 - \text{æ} - u$ (the dimensionless minimum distance between interacting surfaces). It is evident that the force $F(u)$ is greater for a cylindrical pore than for a plane-parallel pore. Meanwhile, the difference in the forces is greater, the greater the value of the parameter æ. It follows from Fig. 6 that the dependence of purification efficiency on the parameter æ is of an extreme nature the function $\lambda(\text{æ})$ has a minimum at $\text{æ} = \text{æ}_{min}$.

However, λ is considerably greater in the case of a membrane with cylindrical channels, while æ_{min} is lower (Fig. 6). Along with this, there is a marked difference in the values of the parameter φ_{min} (Fig. 7). As regards the region of van der Waals force saturation (the range of δ in which λ is independent of the gap size δ), it is nearly the same for both cases (Fig. 8).

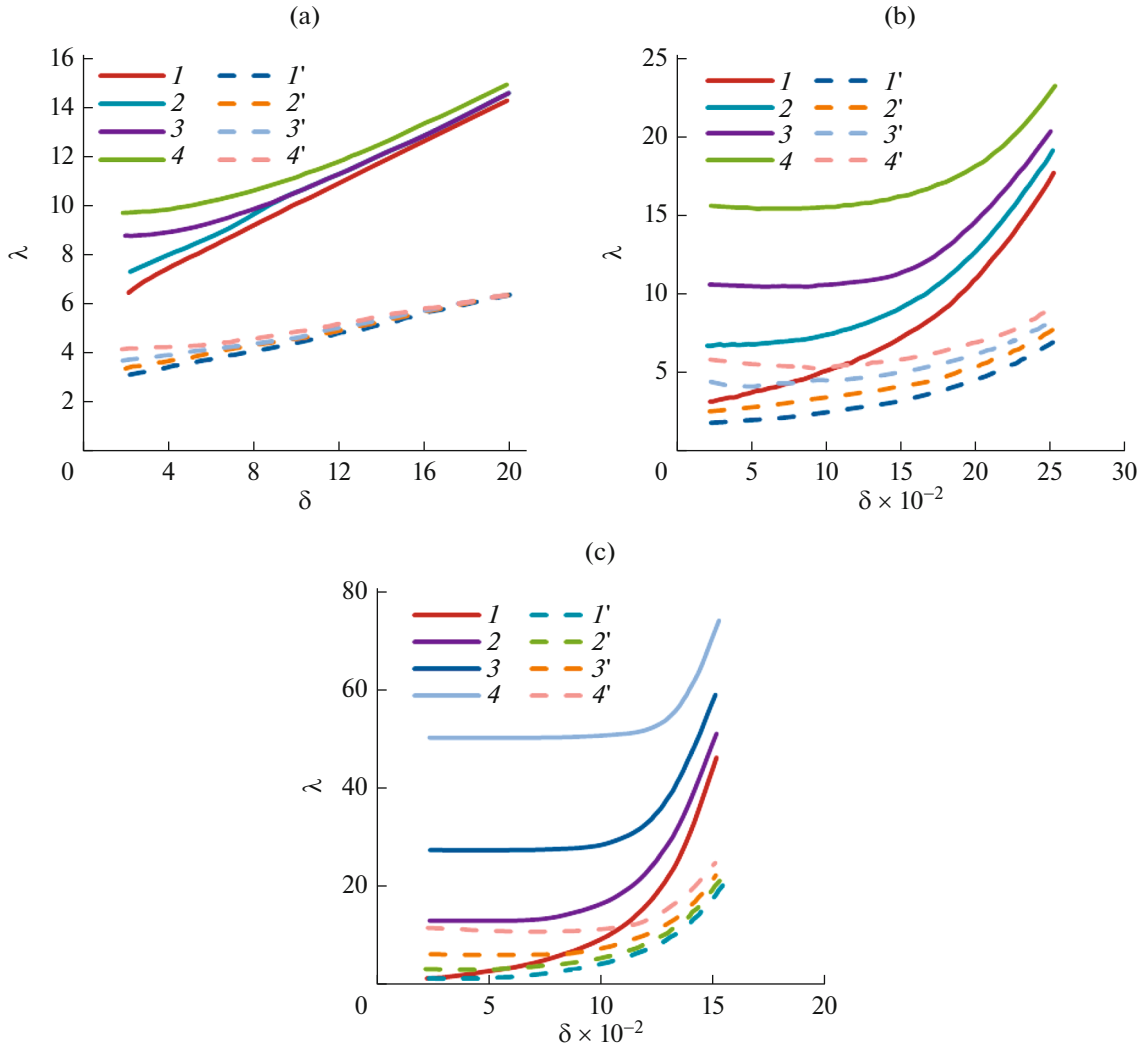

Fig. 8. Dependence of the value of λ on the dimensionless gap size δ. æ: (a) 0.1; (b) 0.5; (c) 0.8; *B*: (*1*, *1'*) 0; (*2*, *2'*) 0.5; (*3*, *3'*) 1.25; (*4*, *4'*) 2.5. The solid line shows the relations corresponding to a membrane with cylindrical channels, while the dashed line shows the relations for a membrane with plane-parallel channels.

CONCLUSIONS

Thus, the calculations show that microfiltration carried out with membranes having plane-parallel channels is qualitatively the same as microfiltration carried out with membranes having cylindrical channels. At the same time, in a quantitative sense, the efficiency of purification (the parameter λ) turns out to be appreciably greater for membranes with cylindrical pores. Meanwhile, the geometry of the cross section of the membrane channels affects both the diffusional transport of particles in pores of the filter (this mechanism makes the main contribution to purification efficiency at $æ < æ_{min}$) and the van der Waals force. The van der Waals force is connected mainly with increases in purification efficiency at $æ > æ_{min}$.

FUNDING

This work was supported by the Ministry of Science and Higher Education of the Russian Federation in the Framework of the Basic Part of the State Task (project no. FSWE-2020-0008).

REFERENCES

1. H. Li, X. Wu, M. Wang, J. Wang, S. Wu, X. Yao, and L. Li, Sep. Purif. Technol. **138**, 41 (2014).
2. M. M. Trubyanov, G. M. Mochalov, V. M. Vorotyntsev, and S. S. Suvorov, Sep. Purif. Technol. **135**, 117 (2014).
3. P. Luis, in *Microfiltration, Ultrafiltration, Nanofiltration, Reverse Osmosis and Forward Osmosis*, 1rd ed., Ed. by B. Van der Bruggen (Elsevier, Oxford, 2018).

4. M. V. Sukhanov, T. I. Storozheva, I. I. Evdokimov, V. G. Pimenov, A. Y. Sozin, and T. V. Kotereva, Inorg. Mater. **53**, 142 (2017).
5. G. G. Devyatykh, Y. E. Elliev, Y. P. Kirillov, and A. Y. Malyshev, Dokl. Akad. Nauk. **367**, 371 (1999).
6. V. M. Vorotyntsev and V. M. Malyshev, Teor. Osn. Khim. Tekhnol. **46**, 563 (2012).
7. V. M. Vorotyntsev and P. N. Drozdov, Sep. Purif. Technol. **22–23**, 367 (2001).
8. G. Z. Ramon and E. M. V Hoek, J. Membr. Sci. **392–393**, 1 (2012).
9. A. V. Vorotyntsev, A. N. Petukhov, M. M. Trubyanov, A. A. Atlaskin, D. A. Makarov, M. S. Sergeeva, I. V. Vorotyntsev, and V. M. Vorotyntsev, Rev. Chem. Eng. **37**, 125 (2019).
10. S. Sinha-Ray, S. Sinha-Ray, A. L. Yarin, and B. Pourdeyhimi, J. Membr. Sci. **485**, 132 (2015).
11. M. Mulder, *Basic Principles of Membrane Technology* (Kluwer Academic, Dordrecht, 1996).
12. V. M. Vorotyntsev, Petr. Chem. **55**, 259 (2015).
13. D. M. Kanani, W. H. Fissel, S. Roy, A. Dabnisheva, A. Fleischman, and A. L. Zidney, J. Membr. Sci. **349**, 405 (2010).
14. D. B. Taulbee, J. Aerosol Sci. **10**, 95 (1979).
15. D. B. Ingham, J. Aerosol Sci. **7**, 373 (1976).
16. B. R. Hurschfeld, H. Brenner, and A. Falade, Physicochem. Hydrodyn. **5**, 99 (1984).
17. P. Ganatos, S. Weinbaum, and R. Pfeffer, J. Fluid Mech. **99**, 739 (1980).
18. B. D. Bowen, S. Levine, and N. Epstein, J. Colloid Interface Sci. **54**, 375 (1976).
19. R. Cheng, T. Zhu, and L. Mao, Microfluid. Nanofluid. **16**, 1143 (2013).
20. P. Talebizadehsardari, H. Rahimzadeh, G. Ahmadi, K. Inthavong, M. M. Keshtkar, and M. A. Moghimi, Adv. Powder Technol. **31**, 3134 (2020).
21. F. London, Trans. Faraday Soc. **33**, 8 (1937).
22. B. V. Derjaguin, I. I. Abrikosova, and E. M. Lifshitz, Q. Rev. Chem. Soc. **10**, 295 (1956).
23. J. A. Logan and A. V. Tkachenko, Phys. Rev. E **98**, 032609 (2018).
24. R. Maniero, E. Climent, and P. Bacchin, Chem. Eng. Sci. **71**, 409 (2012).
25. Y. Gao, K. Zhong, and Y. Kang, Particuology **44**, 159 (2019).
26. X. Hu and D. Lu, Chin. J. Chem. Eng. **27**, 1439 (2019).
27. E. M. Lifshitz and L. P. Pitaevski, *Physical Kinetics* (Pergamon Press, Oxford, 1981).
28. H. Brenner, Chem. Eng. Sci. **16**, 242 (1961).
29. G. Boccardo, D. L. Marchisio, and R. Sethi, J. Colloid Interface Sci. **417**, 227 (2014).
30. D. Alghalibi, W. Fornari, M. E. Rosti, and L. Brandt, Int. J. Multiphas Flow **129**, 103291 (2020).
31. H. C. Hamaker, Physica **4**, 1058 (1937).
32. B. V. Derjaguin, N. V. Churaev, and V. M. Muller, *Surface Forces* (Nauka, Moscow, 1985) [in Russian].
33. H. Sonntag and K. Strenge, *Koagulation und Stabilität Disperser Systeme* (VEB Deutscher Verlag der Wissenschaften, Berlin, 1970).
34. J. Happel and H. Brenner, *Low Reynolds Number Hydrodynamics* (Springer, Dordrecht, 1983).
35. T. Brock, *Membrane Filtration: A User's Guide and Reference Manual* (Science Technical Incorporation, Madison, 1983).
36. Yu. I. Dytnerskii, *Baromembrane Processes* (Khimiya, Moscow, 1986).
37. G. N. Flerov, Vestn. Akad. Nauk SSSR **4**, 35 (1984).
38. P. Yu. Apel, Nucl. Tracks **6**, 115 (1982).
39. Yu. N. Kao, Y. Wang, R. Pfeffer, and S. Weinbaum, J. Colloid Interface Sci. **121**, 543 (1988).
40. G. G. Devyatykh, V. M. Vorotyntsev, Yu. S. Chertkov, and V. A. Dozorov, Vys. Veshch. **3**, 44 (1988).
41. I. S. Gradshtein and I. M. Ryzhik, *Tables of Integrals, Sums, Series and Products* (Fizmatgiz, Moscow, 1963) [in Russian].
42. B. Derjaguin, Kolloid-Z. **69**, 155 (1934).
43. A. S. Dukhin and A. G. Us'yarov, Kolloidn. Zh. **49**, 1055 (1987).